

# $B \rightarrow K_1 \ell^+ \ell^-$ Decays in a Family Non-universal $Z'$ Model

Ying Li\*, Juan Hua

*Department of Physics, Yantai University, Yantai 264-005, China*

Kwei-Chou Yang

*Department of Physics, Chung Yuan Christian University, Chung-Li, Taiwan 320, Republic of China*

(Dated: August 8, 2018)

The implications of the family non-universal  $Z'$  model in the  $B \rightarrow K_1(1270, 1400)\ell^+\ell^-$  ( $\ell = e, \mu, \tau$ ) decays are explored, where the mass eigenstates  $K_1(1270, 1400)$  are the mixtures of  $^1P_1$  and  $^3P_1$  states with the mixing angle  $\theta$ . In this work, considering the  $Z'$  boson and setting the mixing angle  $\theta = (-34 \pm 13)^\circ$ , we analyze the branching ratio, the dilepton invariant mass spectrum, the normalized forward-backward asymmetry and lepton polarization asymmetries of each decay mode. We find that all observables of  $B \rightarrow K_1(1270)\mu^+\mu^-$  are sensitive to the  $Z'$  contribution. Moreover, the observables of  $B \rightarrow K_1(1400)\mu^+\mu^-$  are relatively strong  $\theta$ -dependence; thus, the  $Z'$  contribution will be buried by the uncertainty of the mixing angle  $\theta$ . Furthermore, the zero crossing position in the FBA spectrum of  $B \rightarrow K_1(1270)\mu^+\mu^-$  at low dilepton mass will move to the positive direction with  $Z'$  contribution. For the tau modes, the effects of  $Z'$  are not remarkable due to the small phase space. These results could be tested in the running LHC-b experiment and Super-B factory.

## I. INTRODUCTION

The flavor changing neutral currents (FCNC)  $b \rightarrow s\ell^+\ell^-$  ( $\ell = e, \mu, \tau$ ), forbidden in the standard model (SM) at the tree level, are very sensitive to the flavor structure of the SM and to the new physics (NP) beyond the SM. The rare decays  $B \rightarrow K_1\ell^+\ell^-$  involving axial-vector strange mesons, also induced by  $b \rightarrow s\ell^+\ell^-$ , have been the subjects of many theoretical studies in the frame work of the SM [1–4] and some NP models, such as universal extra dimension [5], models involving supersymmetry [6] and the fourth-generation fermions [7]. Generally, these semileptonic decays provide us with a wealth of information with a number of physical observables, such as branching ratio, dilepton invariant mass spectrum, the forward backward asymmetry, lepton polarization asymmetry and other distributions of interest, which play important roles in testing SM and are regarded as probes of possible NP models.

In the quark model, two lowest nonets of  $J^P = 1^+$  axial-vector mesons are usually expected to be the orbitally excited  $q\bar{q}'$  states. In the context of the spectroscopic notation  $n^{2S+1}L_J$ , where the radial excitation is denoted by the principal number  $n$ , there are two types of lowest  $p$ -wave meson, namely,  $^3P_1$  and  $^1P_1$ . The two nonets have distinctive  $C$  quantum numbers,  $C = +$  or  $C = -$ , respectively. Experimentally, the  $J^{PC} = 1^{++}$  nonet consists of  $a_1(1260)$ ,  $f_1(1285)$ ,  $f_1(1420)$ , and  $K_{1A}$ , while the  $1^{+-}$  nonet contains  $b_1(1235)$ ,  $h_1(1170)$ ,  $h_1(1380)$  and  $K_{1B}$ . The physical mass eigenstates  $K_1(1270)$  and  $K_1(1400)$  are mixtures of  $K_{1A}$  and  $K_{1B}$  states owing to the mass difference of the strange and non-strange light quarks, and the relation could be written as:

$$\begin{pmatrix} |\bar{K}_1(1270)\rangle \\ |\bar{K}_1(1400)\rangle \end{pmatrix} = M \begin{pmatrix} |\bar{K}_{1A}\rangle \\ |\bar{K}_{1B}\rangle \end{pmatrix}, \quad \text{with} \quad M = \begin{pmatrix} \sin \theta & \cos \theta \\ \cos \theta & -\sin \theta \end{pmatrix}. \quad (1)$$

\* liying@ytu.edu.cn

In the past few years, many attempts have been made to constrain the mixing angle  $\theta$  [8–11]. In this study, we will use  $\theta = -(34 \pm 13)^\circ$  for numerical calculations, which has been extracted from  $B \rightarrow K_1(1270)\gamma$  and  $\tau \rightarrow K_1(1270)\nu_\tau$  by one of us in [11], and the minus sign is related to the chosen phase of  $|\bar{K}_{1A}\rangle$  and  $|\bar{K}_{1B}\rangle$ .

To make predictions of these exclusive decays, one requires the additional knowledge about form factors, i.e., the matrix elements of the effective Hamiltonian between initial and final states. This problem, being a part of the nonperturbative sector of QCD, lacks a precise solution. To the best of our knowledge, a number of different approaches had been used to calculate the decay form factors of  $B \rightarrow K_1$  decays, such as QCD sum rules [12], light cone sum rules (LCSRs) [13], perturbative QCD approach [14] and light front quark model [15]. Among them, the results obtained by LCSRs which deal with form factors at small momentum region, are complementary to the lattice approach and have consistence with perturbative QCD and the heavy quark limit. On this point, we will use the results of LCSRs [13] in this work.

In some new physics models,  $Z'$  gauge boson could be naturally derived in certain string constructions [16] and  $E_6$  models [17] by adding additional  $U(1)'$  gauge symmetry [18]. Among many  $Z'$  models, the simplest one is the family non-universal  $Z'$  model. It is of interest to note that in such a model the non-universal  $Z'$  couplings could lead to FCNCs at tree level as well as introduce new weak phases, which could explain the CP asymmetries in the current high energy experiments. The effects of  $Z'$  in the  $B$  sector have been investigated in the literature, for example see Ref. [19–21]. The recent detailed review is Ref. [22]. In Ref. [21], Chang *et al* obtained the explicit picture of  $Z'$  couplings with the data of  $\bar{B}_s - B_s$  mixing,  $B \rightarrow K^{(*)}\ell^+\ell^-$ ,  $B \rightarrow \mu^+\mu^-$ ,  $B \rightarrow K\pi$  and inclusive decays  $B \rightarrow X_s\ell^+\ell^-$ . So, it should be interesting to explore the discrepancy of observables between predictions of SM and those of the family non-universal  $Z'$  model. Motivated by this, we shall address the effects of the  $Z'$  boson in the rare decays  $B \rightarrow K_1\ell^+\ell^-$ .

In experiments,  $B \rightarrow K_1\ell^+\ell^-$  have not yet been measured, but are expected to be observed at LHC-b [23] and Super-B factory [24]. In particular, it is estimated that there will be almost 8000  $B \rightarrow K^*\mu^+\mu^-$  events with an integrated luminosity of  $2fb^{-1}$  in the LHC-b experiment [23, 25]. Although the branching ratio of  $B \rightarrow K_1(1270)\mu^+\mu^-$  calculated in [1] is one order of magnitude smaller than the experimentally measured value of  $B \rightarrow K^*\mu^+\mu^-$  [26], we still expect the significant number of events for this decay.

The remainder of this paper is organized as follows: in section 2, we introduce the effective Hamiltonian responsible for the  $b \rightarrow s\ell^+\ell^-$  transition in both SM and  $Z'$  model. Using the effective Hamiltonian and  $B \rightarrow K_1$  form factors, we obtain the branching ratios as well as various related physical observables. In section 3, we numerically analyze the considered observables of  $B \rightarrow K_1\ell^+\ell^-$ . This section also includes a comparison of the results obtained in  $Z'$  model with those predicted by the SM. We will summarize this work in the last section.

## II. ANALYTIC FORMULAS

### A. The Effective Hamiltonian for $b \rightarrow s$ transition in SM

By integrating out the heavy degrees of freedom including top quark,  $W^\pm$  and  $Z$  bosons above scale  $\mu = O(m_b)$ , the effective Hamiltonian responsible for the  $b \rightarrow s\ell^+\ell^-$  transitions is given as [27, 28]:

$$H_{eff}(b \rightarrow s\ell^+\ell^-) = -\frac{G_F}{2\sqrt{2}}V_{tb}V_{ts}^*\sum_{i=1}^{10}C_i(\mu)O_i(\mu), \quad (2)$$

where we have neglected the terms proportional to  $V_{ub}V_{us}^*$  on account of  $|V_{ub}V_{us}^*/V_{tb}V_{ts}^*| < 0.02$ . The local operators can be found in [27]. Specifically, the operators  $O_9$  and  $O_{10}$  are given as

$$O_9 = \frac{e^2}{g_s^2} (\bar{s}\gamma_\mu P_L b) (\bar{\ell}\gamma^\mu \ell), \quad O_{10} = \frac{e^2}{g_s^2} (\bar{s}\gamma_\mu P_L b) (\bar{\ell}\gamma^\mu \gamma_5 \ell). \quad (3)$$

In SM, the Wilson coefficients  $C_i$  at scale  $\mu = m_b$  calculated in the naive dimensional regularization (NDR) scheme [27] are collected in Table I. It should be stressed that for  $b \rightarrow s\ell^+\ell^-$  processes, the quark decay amplitude can also receive additional

TABLE I: The SM Wilson coefficients at the scale  $\mu = m_b$ .

| $C_1(m_b)$ | $C_2(m_b)$ | $C_3(m_b)$ | $C_4(m_b)$ | $C_5(m_b)$ | $C_6(m_b)$ | $C_7^{\text{eff}}(m_b)$ | $C_9^{\text{eff}}(m_b) - Y(q^2)$ | $C_{10}(m_b)$ |
|------------|------------|------------|------------|------------|------------|-------------------------|----------------------------------|---------------|
| -0.274     | 1.007      | -0.004     | 0.076      | 0.000      | 0.001      | -0.302                  | 4.094                            | -4.193        |

contributions from the matrix element of four-quark operators,  $\sum_{i=1}^6 \langle \ell^+\ell^- s | O_i | b \rangle$ , which are usually absorbed into the effective Wilson coefficients. The effective coefficients  $C_{7,9}^{\text{eff}}$  in Table I are defined respectively as [29]

$$\begin{aligned} C_7^{\text{eff}} &= \frac{4\pi}{\alpha_s} C_7 - \frac{1}{3} C_3 - \frac{4}{9} C_4 - \frac{20}{3} C_5 - \frac{80}{9} C_6, \\ C_9^{\text{eff}} &= \frac{4\pi}{\alpha_s} C_9 + Y_{SD}(z, \hat{s}) + Y_{LD}(z, \hat{s}), \end{aligned} \quad (4)$$

with definitions  $z = m_c/m_b$ ,  $\hat{s} = q^2/m_b^2$ .  $Y_{SD}(z, \hat{s})$  represents the short-distance contributions from four-quark operators far away from the  $c\bar{c}$  resonances regions, which can be calculated reliably in the perturbative theory. On the contrary, the long-distance contributions  $Y_{LD}(z, \hat{s})$  from four-quark operators near the  $c\bar{c}$  resonances cannot be calculated and are usually parameterized in the form of a phenomenological Breit-Wigner formula. Currently, the light-cone distribution amplitudes of the axial-vector mesons actually have not yet been well studied, since contributions of two axial-vector mesons in the hadronic dispersion relation cannot be separated in all cases. Moreover, the width effect of axial-vector meson is so large that the traditional approach like the sum rules cannot deal with it effectively. The manifest expressions and discussions for  $Y_{SD}(z, \hat{s})$  and  $Y_{LD}(z, \hat{s})$ , are referred to Ref. [30]. Since the contribution of long distance can be vetoed effectively in the experimental side, we will not discuss it in the current work. Furthermore, for the  $C_7^{\text{eff}}$ , we here also ignore the long-distance contribution of the charm quark loop, which is suppressed heavily by the Breit-Wigner factor.

## B. Family Non-universal $Z'$ Model and Parameter Constraint

As stated before, in the family non-universal  $Z'$  model, there exists the flavor changing neutral current even at the tree level due to the non-diagonal chiral coupling matrix. Assuming that the couplings of right-handed quark flavors with  $Z'$  boson are diagonal and ignoring  $Z - Z'$  mixing, the  $Z'$  part of the effective Hamiltonian for  $b \rightarrow s\ell^+\ell^-$  can be written as [19–21]

$$H_{eff}^{Z'}(b \rightarrow s\ell^+\ell^-) = -\frac{2G_F}{\sqrt{2}} V_{tb}V_{ts}^* \left[ -\frac{B_{sb}^L B_{\ell\ell}^L}{V_{tb}V_{ts}^*} (\bar{s}b)_{V-A} (\bar{\ell}\ell)_{V-A} - \frac{B_{sb}^L B_{\ell\ell}^R}{V_{tb}V_{ts}^*} (\bar{s}b)_{V-A} (\bar{\ell}\ell)_{V+A} \right] + \text{h.c.} \quad (5)$$

To match the effective Hamiltonian in SM, as shown in Eq.(2), the above equation is reformulated as

$$H_{eff}^{Z'}(b \rightarrow s\ell^+\ell^-) = -\frac{4G_F}{\sqrt{2}} V_{tb}V_{ts}^* [\Delta C_9' O_9 + \Delta C_{10}' O_{10}] + \text{h.c.}, \quad (6)$$

with

$$\Delta C'_9(m_W) = -\frac{g_s^2}{e^2} \frac{B_{sb}^L}{V_{tb}V_{ts}^*} (B_{\ell\ell}^L + B_{\ell\ell}^R), \quad \Delta C'_{10}(m_W) = +\frac{g_s^2}{e^2} \frac{B_{sb}^L}{V_{tb}V_{ts}^*} (B_{\ell\ell}^L - B_{\ell\ell}^R), \quad (7)$$

where  $B_{sb}^L$  and  $B_{il}^{L,R}$  denote the effective chiral  $Z'$  couplings to quarks and leptons. Therefore, the  $Z'$  contributions can be represented as modifications of the Wilson coefficients of the corresponding semileptonic operators, i.e.,  $C'_{9,10}(m_W) = C_{9,10}^{SM}(m_W) + \Delta C'_{9,10}(m_W)$ . The running from  $m_W$  scale down to  $m_b$  is the same as that of SM [31, 32], and we had ignored the evolution effect from  $m_{Z'}$  to  $m_W$  here. Numerically, with the central values of the inputs, we get

$$C'_9(m_b) = 0.0682 - 28.82 \frac{B_{sb}^L}{V_{tb}V_{ts}^*} S_{\ell\ell}, \quad C'_{10}(m_b) = -0.0695 + 28.82 \frac{B_{sb}^L}{V_{tb}V_{ts}^*} D_{\ell\ell}, \quad (8)$$

where  $S_{\ell\ell} = (B_{\ell\ell}^L + B_{\ell\ell}^R)$  and  $D_{\ell\ell} = (B_{\ell\ell}^L - B_{\ell\ell}^R)$ .

### C. Form Factor

Following the definitions in Ref. [13], the  $\bar{B}(p_B) \rightarrow \bar{K}_1(p_{K_1}, \lambda)$  form factors could be parameterized as

$$\begin{aligned} \langle \bar{K}_1(p_{K_1}, \lambda) | \bar{s} \gamma_\mu (1 - \gamma_5) b | \bar{B}(p_B) \rangle &= -i \frac{2}{m_B + m_{K_1}} \varepsilon_{\mu\nu\rho\sigma} \varepsilon_{(\lambda)}^{*\nu} p_B^\rho p_{K_1}^\sigma A^{K_1}(q^2) + 2m_{K_1} \frac{\varepsilon_{(\lambda)}^* \cdot p_B}{q^2} q_\mu \left[ V_3^{K_1}(q^2) - V_0^{K_1}(q^2) \right] \\ &\quad - \left[ (m_B + m_{K_1}) \varepsilon_\mu^{(\lambda)*} V_1^{K_1}(q^2) - (p_B + p_{K_1})_\mu (\varepsilon_{(\lambda)}^* \cdot p_B) \frac{V_2^{K_1}(q^2)}{m_B + m_{K_1}} \right], \end{aligned} \quad (9)$$

$$\begin{aligned} \langle \bar{K}_1(p_{K_1}, \lambda) | \bar{s} \sigma_{\mu\nu} q^\nu (1 + \gamma_5) b | \bar{B}(p_B) \rangle &= 2T_1^{K_1}(q^2) \varepsilon_{\mu\nu\rho\sigma} \varepsilon_{(\lambda)}^{*\nu} p_B^\rho p_{K_1}^\sigma - iT_3^{K_1}(q^2) (\varepsilon_{(\lambda)}^* \cdot q) \left[ q_\mu - \frac{q^2}{m_B^2 - m_{K_1}^2} (p_{K_1} + p_B)_\mu \right] \\ &\quad - iT_2^{K_1}(q^2) \left[ (m_B^2 - m_{K_1}^2) \varepsilon_{*\mu}^{(\lambda)} - (\varepsilon_{(\lambda)}^* \cdot q) (p_B + p_{K_1})_\mu \right], \end{aligned} \quad (10)$$

with  $q \equiv p_B - p_{K_1}$ ,  $\gamma_5 \equiv i\gamma^0\gamma^1\gamma^2\gamma^3$ , and  $\varepsilon^{0123} = -1$ . In the context of equation of motion, the form factors satisfy the following relations,

$$\begin{aligned} V_3^{K_1}(0) &= V_0^{K_1}(0), \quad T_1^{K_1}(0) = T_2^{K_1}(0), \\ V_3^{K_1}(q^2) &= \frac{m_B + m_{K_1}}{2m_{K_1}} V_1^{K_1}(q^2) - \frac{m_B - m_{K_1}}{2m_{K_1}} V_2^{K_1}(q^2). \end{aligned} \quad (11)$$

Because the  $K_1(1270)$  and  $K_1(1400)$  are the mixing states of the  $K_{1A}$  and  $K_{1B}$ , the  $\bar{B} \rightarrow \bar{K}_1$  form factors can be parameterized as:

$$\begin{pmatrix} \langle \bar{K}_1(1270) | \bar{s} \gamma_\mu (1 - \gamma_5) b | \bar{B} \rangle \\ \langle \bar{K}_1(1400) | \bar{s} \gamma_\mu (1 - \gamma_5) b | \bar{B} \rangle \end{pmatrix} = M \begin{pmatrix} \langle \bar{K}_{1A} | \bar{s} \gamma_\mu (1 - \gamma_5) b | \bar{B} \rangle \\ \langle \bar{K}_{1B} | \bar{s} \gamma_\mu (1 - \gamma_5) b | \bar{B} \rangle \end{pmatrix}, \quad (12)$$

$$\begin{pmatrix} \langle \bar{K}_1(1270) | \bar{s} \sigma_{\mu\nu} q^\nu (1 + \gamma_5) b | \bar{B} \rangle \\ \langle \bar{K}_1(1400) | \bar{s} \sigma_{\mu\nu} q^\nu (1 + \gamma_5) b | \bar{B} \rangle \end{pmatrix} = M \begin{pmatrix} \langle \bar{K}_{1A} | \bar{s} \sigma_{\mu\nu} q^\nu (1 + \gamma_5) b | \bar{B} \rangle \\ \langle \bar{K}_{1B} | \bar{s} \sigma_{\mu\nu} q^\nu (1 + \gamma_5) b | \bar{B} \rangle \end{pmatrix}, \quad (13)$$

with the mixing matrix  $M$  being given in Eq. (1). Thus the form factors  $A^{K_1}$ ,  $V_{0,1,2}^{K_1}$  and  $T_{1,2,3}^{K_1}$  satisfy following relations:

$$\begin{pmatrix} A^{K_1(1270)} / (m_B + m_{K_1(1270)}) \\ A^{K_1(1400)} / (m_B + m_{K_1(1400)}) \end{pmatrix} = M \begin{pmatrix} A^{K_{1A}} / (m_B + m_{K_{1A}}) \\ A^{K_{1B}} / (m_B + m_{K_{1B}}) \end{pmatrix}, \quad (14)$$

$$\begin{pmatrix} (m_B + m_{K_1(1270)}) V_1^{K_1(1270)} \\ (m_B + m_{K_1(1400)}) V_1^{K_1(1400)} \end{pmatrix} = M \begin{pmatrix} (m_B + m_{K_{1A}}) V_1^{K_{1A}} \\ (m_B + m_{K_{1B}}) V_1^{K_{1B}} \end{pmatrix}, \quad (15)$$

TABLE II: Form factors for  $B \rightarrow K_{1A}, K_{1B}$  transitions obtained in the LCSRs calculation [13] are fitted to the 3-parameter form in Eq. (21).

| $F$             | $F(0)$ | $a$  | $b$  | $F$             | $F(0)$ | $a$   | $b$   |
|-----------------|--------|------|------|-----------------|--------|-------|-------|
| $V_1^{BK_{1A}}$ | 0.34   | 0.64 | 0.21 | $V_1^{BK_{1B}}$ | -0.29  | 0.73  | 0.07  |
| $V_2^{BK_{1A}}$ | 0.41   | 1.51 | 1.18 | $V_2^{BK_{1B}}$ | -0.17  | 0.92  | 0.86  |
| $V_0^{BK_{1A}}$ | 0.22   | 2.40 | 1.78 | $V_0^{BK_{1B}}$ | -0.45  | 1.34  | 0.69  |
| $A^{BK_{1A}}$   | 0.45   | 1.60 | 0.97 | $A^{BK_{1B}}$   | -0.37  | 1.72  | 0.91  |
| $T_1^{BK_{1A}}$ | 0.31   | 2.01 | 1.50 | $T_1^{BK_{1B}}$ | -0.25  | 1.59  | 0.79  |
| $T_2^{BK_{1A}}$ | 0.31   | 0.63 | 0.39 | $T_2^{BK_{1B}}$ | -0.25  | 0.38  | -0.76 |
| $T_3^{BK_{1A}}$ | 0.28   | 1.36 | 0.72 | $T_3^{BK_{1B}}$ | -0.11  | -1.61 | 10.2  |

$$\begin{pmatrix} V_2^{K_1(1270)}/(m_B + m_{K_1(1270)}) \\ V_2^{K_1(1400)}/(m_B + m_{K_1(1400)}) \end{pmatrix} = M \begin{pmatrix} V_2^{K_{1A}}/(m_B + m_{K_{1A}}) \\ V_2^{K_{1B}}/(m_B + m_{K_{1B}}) \end{pmatrix}, \quad (16)$$

$$\begin{pmatrix} m_{K_1(1270)} V_0^{K_1(1270)} \\ m_{K_1(1400)} V_0^{K_1(1400)} \end{pmatrix} = M \begin{pmatrix} m_{K_{1A}} V_0^{K_{1A}} \\ m_{K_{1B}} V_0^{K_{1B}} \end{pmatrix}, \quad (17)$$

$$\begin{pmatrix} T_1^{K_1(1270)} \\ T_1^{K_1(1400)} \end{pmatrix} = M \begin{pmatrix} T_1^{K_{1A}} \\ T_1^{K_{1B}} \end{pmatrix}, \quad (18)$$

$$\begin{pmatrix} (m_B^2 - m_{K_1(1270)}^2) T_2^{K_1(1270)} \\ (m_B^2 - m_{K_1(1400)}^2) T_2^{K_1(1400)} \end{pmatrix} = M \begin{pmatrix} (m_B^2 - m_{K_{1A}}^2) T_2^{K_{1A}} \\ (m_B^2 - m_{K_{1B}}^2) T_2^{K_{1B}} \end{pmatrix}, \quad (19)$$

$$\begin{pmatrix} T_3^{K_1(1270)} \\ T_3^{K_1(1400)} \end{pmatrix} = M \begin{pmatrix} T_3^{K_{1A}} \\ T_3^{K_{1B}} \end{pmatrix}, \quad (20)$$

where we have assumed  $p_{K_1(1270), K_1(1400)}^\mu \simeq p_{K_{1A}}^\mu \simeq p_{K_{1B}}^\mu$  for simplicity. For the form factors, we will use results calculated with LCSRs [13], which are exhibited in Table II. In the whole kinematical region, the dependence of each form factor on momentum transfer  $q^2$  is parameterized in the double-pole form:

$$F(q^2) = \frac{F(0)}{1 - a(q^2/m_B^2) + b(q^2/m_B^2)^2}. \quad (21)$$

And the nonperturbative parameters  $a_i$  and  $b_i$  can be fitted by the magnitudes of form factors corresponding to the small momentum transfer calculated in the LCSRs approach.

#### D. Formulas of Observables

With the same convention and notation as [1], the dilepton invariant mass spectrum of the lepton pair for the  $\bar{B} \rightarrow \bar{K}_1 \ell^+ \ell^-$  decay is given as

$$\frac{d\Gamma(\bar{B} \rightarrow \bar{K}_1 \ell^+ \ell^-)}{d\hat{s}} = \frac{G_F^2 \alpha_{\text{em}}^2 m_B^5}{2^{10} \pi^5} |V_{tb} V_{ts}^*|^2 \hat{u}(\hat{s}) \Delta \quad (22)$$

and

$$\begin{aligned} \Delta = & \frac{|\mathcal{A}^{K_1}|^2}{3} \hat{s} \lambda \left( 1 + 2 \frac{\hat{m}_\ell^2}{\hat{s}} \right) + |\mathcal{E}^{K_1}|^2 \hat{s} \frac{\hat{u}(\hat{s})^2}{3} \\ & + \frac{1}{4 \hat{m}_{K_1}^2} \left[ |\mathcal{B}^{K_1}|^2 \left( \lambda - \frac{\hat{u}(\hat{s})^2}{3} + 8 \hat{m}_{K_1}^2 (\hat{s} + 2 \hat{m}_\ell^2) \right) + |\mathcal{F}^{K_1}|^2 \left( \lambda - \frac{\hat{u}(\hat{s})^2}{3} + 8 \hat{m}_{K_1}^2 (\hat{s} - 4 \hat{m}_\ell^2) \right) \right] \end{aligned}$$

$$\begin{aligned}
& + \frac{\lambda}{4\hat{m}_{K_1}^2} \left[ |\mathcal{C}^{K_1}|^2 \left( \lambda - \frac{\hat{u}(\hat{s})^2}{3} \right) + |\mathcal{G}^{K_1}|^2 \left( \lambda - \frac{\hat{u}(\hat{s})^2}{3} + 4\hat{m}_\ell^2(2 + 2\hat{m}_{K_1}^2 - \hat{s}) \right) \right] \\
& - \frac{1}{2\hat{m}_{K_1}^2} \left[ \text{Re}(\mathcal{B}^{K_1} \mathcal{C}^{K_1*}) \left( \lambda - \frac{\hat{u}(\hat{s})^2}{3} \right) (1 - \hat{m}_{K_1}^2 - \hat{s}) + \text{Re}(\mathcal{F}^{K_1} \mathcal{G}^{K_1*}) \left( \left( \lambda - \frac{\hat{u}(\hat{s})^2}{3} \right) (1 - \hat{m}_{K_1}^2 - \hat{s}) + 4\hat{m}_\ell^2 \lambda \right) \right] \\
& - 2 \frac{\hat{m}_\ell^2}{\hat{m}_{K_1}^2} \lambda \left[ \text{Re}(\mathcal{F}^{K_1} \mathcal{H}^{K_1*}) - \text{Re}(\mathcal{G}^{K_1} \mathcal{H}^{K_1*}) (1 - \hat{m}_{K_1}^2) \right] + \frac{\hat{m}_\ell^2}{\hat{m}_{K_1}^2} \hat{s} \lambda |\mathcal{H}^{K_1}|^2.
\end{aligned} \tag{23}$$

with  $\hat{p} = p/m_B$ ,  $\hat{p}_B = p_B/m_B$ ,  $\hat{q} = q/m_B$ ,  $\hat{m}_{K_1} = m_{K_1}/m_B$ , and  $p = p_B + p_{K_1}$ ,  $q = p_B - p_{K_1} = p_+ + p_-$ . The auxiliary functions  $\mathcal{A}^{K_1}(\hat{s}), \dots, \mathcal{H}^{K_1}(\hat{s})$  are defined in Ref.[11], and we list them in the Appendix for convenience. Here, we also choose  $\hat{s} = \hat{q}^2$  and  $\hat{u} \equiv (\hat{p}_B - \hat{p}_-)^2 - (\hat{p}_B - \hat{p}_+)^2$  as the two independent parameters, which are bounded as  $4\hat{m}_\ell^2 \leq \hat{s} \leq (1 - \hat{m}_{K_1})^2$  and  $-\hat{u}(\hat{s}) \leq \hat{u} \leq \hat{u}(\hat{s})$ , with  $\hat{u}(\hat{s}) \equiv \sqrt{\lambda(1 - 4\hat{m}_\ell^2/\hat{s})}$ ,  $\lambda \equiv 1 + \hat{m}_{K_1}^2 + \hat{s}^2 - 2\hat{s} - 2\hat{m}_{K_1}^2(1 + \hat{s})$ .

The differential forward-backward asymmetry of the  $\bar{B} \rightarrow \bar{K}_1 \ell^+ \ell^-$  decay is defined as

$$\frac{dA_{\text{FB}}}{d\hat{s}} \equiv \int_0^{\hat{u}(\hat{s})} d\hat{u} \frac{d^2\Gamma}{d\hat{u}d\hat{s}} - \int_{-\hat{u}(\hat{s})}^0 d\hat{u} \frac{d^2\Gamma}{d\hat{u}d\hat{s}}. \tag{24}$$

Furthermore, the normalized forward-backward asymmetry, which is more useful in the experimental side, can be written in terms of quantities as

$$\frac{d\bar{A}_{\text{FB}}}{d\hat{s}} \equiv \frac{dA_{\text{FB}}}{d\hat{s}} \bigg/ \frac{d\Gamma}{d\hat{s}} \equiv \hat{u}(\hat{s}) \hat{s} \left[ \text{Re}(\mathcal{B}^{K_1} \mathcal{C}^{K_1*}) + \text{Re}(\mathcal{A}^{K_1} \mathcal{F}^{K_1*}) \right]. \tag{25}$$

Here, we do not consider the hard spectator corrections since the light-cone distribution amplitudes of  $K_1$  are not precise enough.

At the end of this section, we pay our attentions on obtaining the lepton polarization asymmetries. In the center mass frame of dilepton, the three orthogonal unit vectors could be defined as

$$\hat{e}_L = \vec{p}_+, \quad \hat{e}_N = \frac{\vec{p}_K \times \vec{p}_+}{|\vec{p}_K \times \vec{p}_+|}, \quad \hat{e}_T = \hat{e}_N \times \hat{e}_L, \tag{26}$$

which are related to the spins of leptons by a Lorentz boost. So, the decay width of the  $B \rightarrow K_1 \ell^+ \ell^-$  decay for any spin direction  $\hat{n}$  of the lepton, where  $\hat{n}$  is a unit vector in the dilepton center mass frame, can be written as:

$$\frac{d\Gamma(\hat{n})}{d\hat{s}} = \frac{1}{2} \left( \frac{d\Gamma}{d\hat{s}} \right)_0 [1 + (P_L \hat{e}_L + P_N \hat{e}_N + P_T \hat{e}_T) \cdot \hat{n}]. \tag{27}$$

In the above equation, the subscript "0" denotes the unpolarized decay width, and  $P_L$  and  $P_T$  are the longitudinal and transverse polarization asymmetries in the decay plane, respectively.  $P_N$  is the normal polarization asymmetry in the direction perpendicular to the decay plane. Correspondingly, the lepton polarization asymmetry  $P_i$  ( $i = L, N, T$ ) can be obtained by calculating

$$P_i(\hat{s}) = \frac{d\Gamma(\hat{n} = \hat{e}_i)/d\hat{s} - d\Gamma(\hat{n} = -\hat{e}_i)/d\hat{s}}{d\Gamma(\hat{n} = \hat{e}_i)/d\hat{s} + d\Gamma(\hat{n} = -\hat{e}_i)/d\hat{s}}. \tag{28}$$

After a straightforward calculation, we obtain:

$$\begin{aligned}
P_{L\Delta} &= \sqrt{1 - 4\frac{\hat{m}_\ell^2}{\hat{s}}} \left\{ \frac{2\hat{s}\lambda}{3} \text{Re}(\mathcal{A} \mathcal{C}^{K_1*}) + \frac{(\lambda + 12\hat{m}_{K_1}^2 \hat{s})}{3\hat{m}_{K_1}^2} \text{Re}(\mathcal{B} \mathcal{F}^{K_1*}) \right. \\
&\quad \left. - \frac{\lambda(1 - \hat{m}_{K_1}^2 - \hat{s})}{3\hat{m}_{K_1}^2} \text{Re}(\mathcal{B} \mathcal{G}^{K_1*} + \mathcal{C} \mathcal{F}^{K_1*}) + \frac{\lambda^2}{3\hat{m}_{K_1}^2} \text{Re}(\mathcal{C} \mathcal{G}^{K_1*}) \right\}, \\
P_{N\Delta} &= \frac{-\pi\sqrt{\hat{s}}\hat{u}(\hat{s})}{4\hat{m}_{K_1}} \left\{ \frac{\hat{m}_\ell}{\hat{m}_{K_1}} [\text{Im}(\mathcal{F} \mathcal{G}^{K_1*})(1 + 3\hat{m}_{K_1}^2 - \hat{s}) \right.
\end{aligned} \tag{29}$$

TABLE III: Input parameters

|   |
|---|
| $m_B = 5.279 \text{ GeV}$ , $\tau_{B^-} = 1.638 \times 10^{-12} \text{ sec}$ , $\tau_{B^0} = 1.530 \times 10^{-12} \text{ sec}$ ,             |
| $m_{K_1(1270)} = 1.272 \text{ GeV}$ , $m_{K_1(1400)} = 1.403 \text{ GeV}$ , $m_{K_{1A}} = 1.31 \text{ GeV}$ , $m_{K_{1B}} = 1.34 \text{ GeV}$ |
| $ V_{tb}V_{ts}^*  = 0.0407$ , $m_{b,\text{pole}} = 4.8 \pm 0.2 \text{ GeV}$ , $\alpha_{em} = 1/129$ , $\alpha_s(\mu_h) = 0.3$ ,               |

TABLE IV: Predictions for the non-resonant branching fractions  $\text{Br}(B \rightarrow K_1 \ell^+ \ell^-)(10^{-6})$  in the SM and the non-universal  $Z'$  model. The first errors come from the uncertainty of the  $\theta = (-34 \pm 13)^\circ$  and the second errors are combination of all uncertainties in the  $Z'$  model.

| Mode  | SM                     | S1                              | S2                              | Extreme Limit          |
|---|------------------------|---------------------------------|---------------------------------|------------------------|
| $B^- \rightarrow K_1^-(1270)e^+e^-$                   | $24.1_{-3.6}^{+0.2}$   | $33.7_{-3.5}^{+0.1} \pm 7.4$    | $28.8_{-3.0}^{+0.2} \pm 3.9$    | $49.6_{-5.3}^{+0.1}$   |
| $B^- \rightarrow K_1^-(1270)\mu^+\mu^-$               | $19.7_{-1.8}^{+0.2}$   | $29.1_{-3.5}^{+0.1} \pm 7.4$    | $24.3_{-3.2}^{+0.0} \pm 3.9$    | $44.9_{-4.2}^{+0.2}$   |
| $B^- \rightarrow K_1^-(1270)\tau^+\tau^-$             | $0.8_{-0.2}^{+0.0}$    | $0.7_{-0.1}^{+0.1} \pm 0.3$     | $0.8_{-0.2}^{+0.0} \pm 0.2$     | $1.2_{-0.2}^{+0.0}$    |
| $B^- \rightarrow K_1^-(1400)e^+e^-$                   | $0.9_{+2.2}^{-0.4}$    | $1.2_{+3.0}^{-0.4} \pm 0.3$     | $1.0_{+2.7}^{-0.3} \pm 0.2$     | $1.6_{+4.3}^{-0.4}$    |
| $B^- \rightarrow K_1^-(1400)\mu^+\mu^-$               | $0.5_{+1.6}^{-0.0}$    | $0.8_{+2.4}^{-0.0} \pm 0.2$     | $0.7_{+1.9}^{-0.1} \pm 0.2$     | $1.3_{+3.5}^{-0.1}$    |
| $B^- \rightarrow K_1^-(1400)\tau^+\tau^-$             | $0.01_{+0.04}^{-0.00}$ | $0.01_{+0.04}^{-0.01} \pm 0.01$ | $0.01_{+0.05}^{-0.01} \pm 0.01$ | $0.02_{+0.06}^{-0.02}$ |
| $\bar{B}^0 \rightarrow \bar{K}_1^0(1270)e^+e^-$       | $22.5_{-3.4}^{+0.2}$   | $31.5_{-3.3}^{+0.1} \pm 7.2$    | $26.9_{-2.8}^{+0.2} \pm 3.8$    | $46.3_{-4.6}^{+0.1}$   |
| $\bar{B}^0 \rightarrow \bar{K}_1^0(1270)\mu^+\mu^-$   | $18.4_{-1.7}^{+0.1}$   | $27.2_{-2.5}^{+0.1} \pm 7.2$    | $22.8_{-2.2}^{+0.1} \pm 3.8$    | $41.9_{-3.9}^{+0.2}$   |
| $\bar{B}^0 \rightarrow \bar{K}_1^0(1270)\tau^+\tau^-$ | $0.7_{-0.1}^{+0.0}$    | $0.7_{-0.1}^{+0.0} \pm 0.3$     | $0.7_{-0.1}^{+0.0} \pm 0.2$     | $1.1_{-0.1}^{+0.0}$    |
| $\bar{B}^0 \rightarrow \bar{K}_1^0(1400)e^+e^-$       | $0.8_{+2.2}^{-0.3}$    | $1.1_{+2.8}^{-0.4} \pm 0.2$     | $1.0_{+2.4}^{-0.4} \pm 0.2$     | $1.5_{+3.9}^{-0.3}$    |
| $\bar{B}^0 \rightarrow \bar{K}_1^0(1400)\mu^+\mu^-$   | $0.5_{+1.5}^{-0.0}$    | $0.8_{+2.1}^{-0.1} \pm 0.2$     | $0.6_{+1.8}^{-0.0} \pm 0.2$     | $1.2_{+3.3}^{-0.1}$    |
| $\bar{B}^0 \rightarrow \bar{K}_1^0(1400)\tau^+\tau^-$ | $0.01_{+0.04}^{-0.01}$ | $0.01_{+0.04}^{-0.01} \pm 0.01$ | $0.01_{+0.04}^{-0.01} \pm 0.01$ | $0.02_{+0.06}^{-0.02}$ |

$$+ \text{Im}(\mathcal{F} \mathcal{H}^{K_1^*})(1 - \hat{m}_{K_1}^2 - \hat{s}) - \text{Im}(\mathcal{G} \mathcal{H}^{K_1^*})\lambda] + 2\hat{m}_{K_1}\hat{m}_l [\text{Im}(\mathcal{B} \mathcal{E}^{K_1^*}) + \text{Im}(\mathcal{A} \mathcal{F}^{K_1^*})] \Big\}, \quad (30)$$

$$P_{T\Delta} = \frac{\pi\sqrt{\lambda}\hat{m}_l}{4\sqrt{\hat{s}}} \left\{ 4\hat{s}\text{Re}(\mathcal{A} \mathcal{B}^{K_1^*}) + \frac{(1 - \hat{m}_{K_1}^2 - \hat{s})}{\hat{m}_{K_1}^2} [-\text{Re}(\mathcal{B} \mathcal{F}^{K_1^*}) + (1 - \hat{m}_{K_1}^2)\text{Re}(\mathcal{B} \mathcal{G}^{K_1^*}) + \hat{s}\text{Re}(\mathcal{B} \mathcal{H}^{K_1^*})] \right. \\ \left. + \frac{\lambda}{\hat{m}_{K_1}^2} [\text{Re}(\mathcal{C} \mathcal{F}^{K_1^*}) - (1 - \hat{m}_{K_1}^2)\text{Re}(\mathcal{C} \mathcal{G}^{K_1^*}) - \hat{s}\text{Re}(\mathcal{C} \mathcal{H}^{K_1^*})] \right\}. \quad (31)$$

### III. NUMERICAL RESULTS AND DISCUSSION

In this section, we shall calculate aforementioned observables like the branching ratios (BR), the normalized forward-backward asymmetries (FBA) and lepton polarization asymmetries, as well as their sensitivities to the new physics due to  $Z'$  boson. The input parameters used in the numerical calculations are listed in Table.III. In discussing the  $K_1(1270)$  and  $K_1(1400)$ , we have to draw much attention on the mixing angle  $\theta$  defined in Eq.(1), although many attempts have been done to constrain it. The magnitude of  $\theta$  was estimated to be  $|\theta| \approx 34^\circ \vee 57^\circ$  in Ref. [8],  $35^\circ \leq |\theta| \leq 55^\circ$  in Ref. [9], and  $|\theta| = 37^\circ \vee 58^\circ$  in Ref. [10]. Nevertheless, the sign of the  $\theta$  was yet unknown in above studies. From the studies of  $B \rightarrow K_1(1270)\gamma$  and  $\tau \rightarrow K_1(1270)\nu_\tau$ , one of us recently obtained [11]

$$\theta = -(34 \pm 13)^\circ, \quad (32)$$

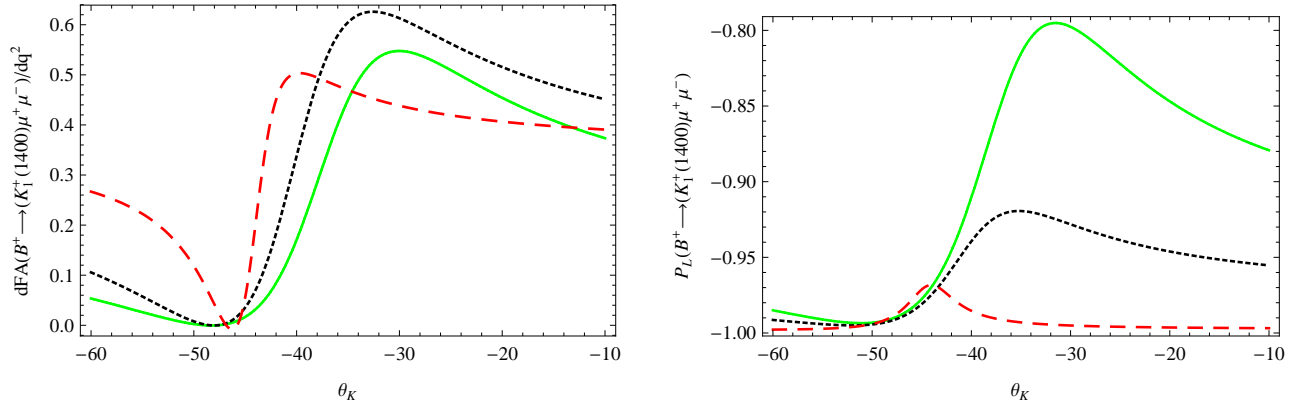


FIG. 1: Normalized differential forward-backward asymmetries (left panel) and longitudinal lepton polarization asymmetry(right panel) of  $B \rightarrow K_1(1400)\mu^+\mu^-$ , as a function of  $\theta$ (in units of degree). The solid, dotted and dashed curves correspond to  $s = 5 \text{ GeV}^2$ ,  $7 \text{ GeV}^2$  and  $12 \text{ GeV}^2$ , respectively.

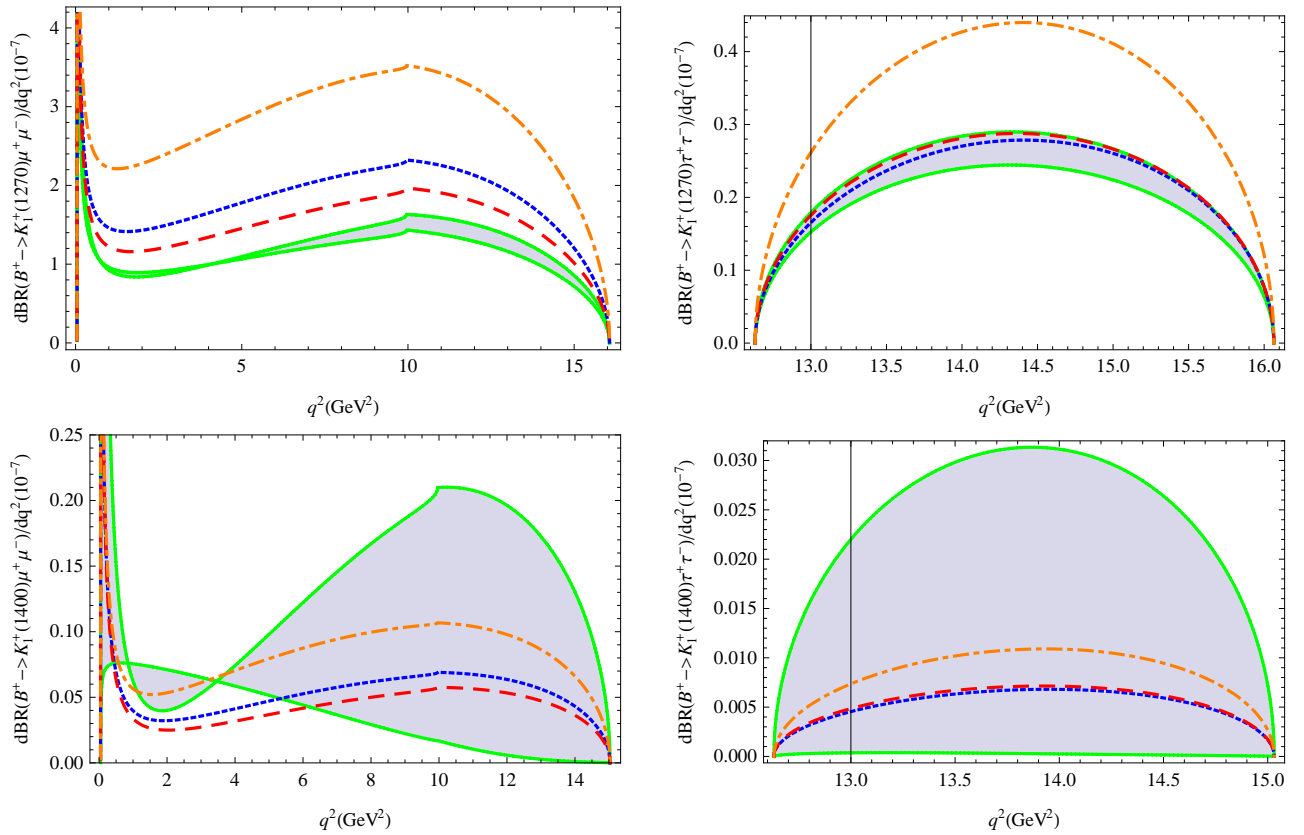
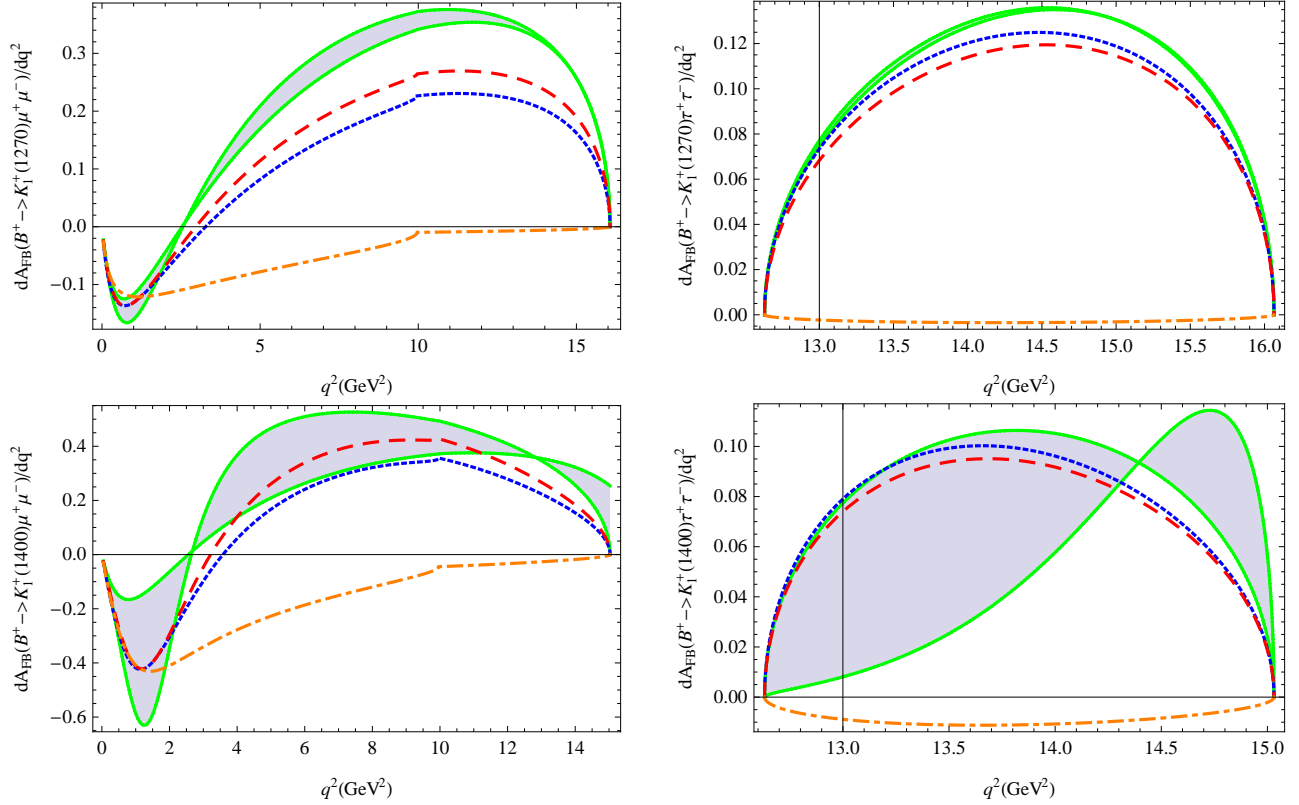


FIG. 2: The differential decay rates  $dBr(B^+ \rightarrow K_1^+ \ell^+ \ell^-)/dq^2$  as functions of  $q^2$ (in units of  $\text{GeV}^2$ ). The central values of inputs are used. The solid (green), and dotted (blue), dashed (red) and dot-dashed (orange) lines represent results from the standard model, S1, S2 and ELV parameters, respectively.



TABLE V: The inputs parameters for the  $Z'$  couplings [21].

|    | $ B_{sb}^L (\times 10^{-3})$ | $\phi_s^L[^\circ]$ | $B_{\mu\mu}^L(\times 10^{-2})$ | $B_{\mu\mu}^R(\times 10^{-2})$ |
|----|------------------------------|--------------------|--------------------------------|--------------------------------|
| S1 | $1.09 \pm 0.22$              | $-72 \pm 7$        | $-4.75 \pm 2.44$               | $1.97 \pm 2.24$                |
| S2 | $2.20 \pm 0.15$              | $-82 \pm 4$        | $-1.83 \pm 0.82$               | $0.68 \pm 0.85$                |

FIG. 3: The normalized differential forward-backward asymmetries for the  $B^+ \rightarrow K_1^+ \ell^+ \ell^-$  decays as functions of  $q^2$  (in units of  $\text{GeV}^2$ ).

where the minus sign of  $\theta$  is related to the chosen phase of  $|\overline{K}_{1A}\rangle$  and  $|\overline{K}_{1B}\rangle$ , and we will use this range in the following discussion.

In Ref. [1], the authors found that in the low  $s$  region, where  $s \approx 2 \text{ GeV}^2$ , the differential decay rate for  $B \rightarrow K_1(1400)\mu^+\mu^-$  with  $\theta = -57^\circ$  is enhanced by about 80% compared with that with  $\theta = -34^\circ$ , whereas the rate for  $B \rightarrow K_1(1270)\mu^+\mu^-$  is not so sensitive to variation of  $\theta$ . After calculation, we emphasize that all observables of  $B \rightarrow K_1(1400)\mu^+\mu^-$  are sensitive to the mixing angle. In Fig.1, for instance, we plot the relations of the normalized forward-backward asymmetry and longitudinal lepton polarization asymmetry of  $B \rightarrow K_1(1400)\mu^+\mu^-$  with  $\theta$  varying from  $-10^\circ$  to  $-60^\circ$ , when  $s = 5 \text{ GeV}^2$  (solid line),  $7 \text{ GeV}^2$  (dotted line) and  $12 \text{ GeV}^2$  (dashed line). With these figures and data, one can constrain the angle in future, as well as cross check the bands from other theories and experiments. Additionally, because of small masses of electron and muon, the invariant mass spectra and branching ratios are almost the same for electron and muon modes. Meanwhile, it is very difficult to measure the electron polarization, so we only consider  $B \rightarrow K_1\mu^+\mu^-$ ,  $K_1\tau^+\tau^-$  except for numerical results in the following discussions.

In Table IV, we again summarize the predictions for branching fractions corresponding to  $\theta = -(34 \pm 13)^\circ$  without consid-

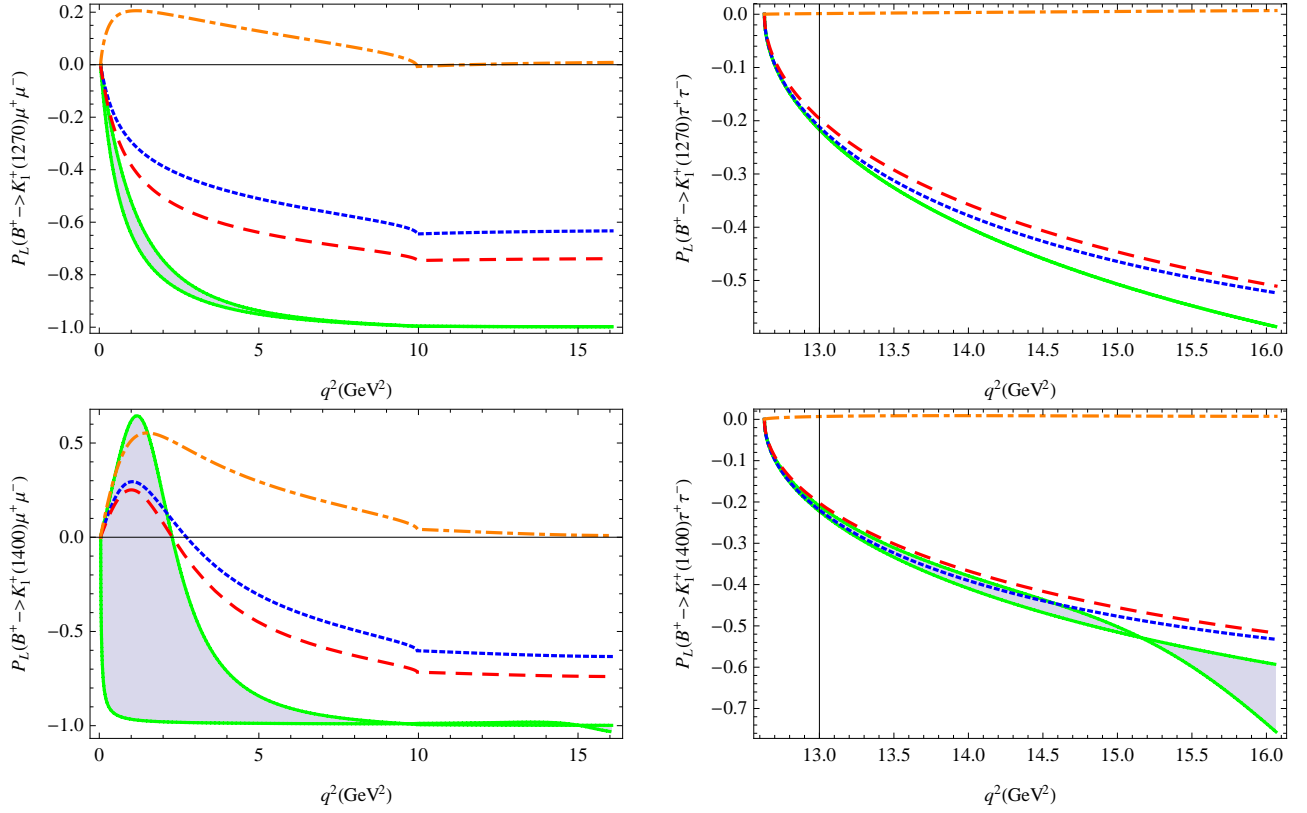


FIG. 4: The longitudinal lepton polarization asymmetries for the  $B^+ \rightarrow K_1^+ \ell^+ \ell^-$  decays as functions of  $q^2$  (in units of  $\text{GeV}^2$ ).

ering the uncertainties taken by the form factors, which have been discussed in detail in Ref. [1]. The negligible disparities between our results and those of Ref.[1] are from the difference of Wilson coefficients. From the table, we note that the branching ratios of  $B \rightarrow K_1(1270)\ell^+\ell^-$  are not sensitive to the mixing angle  $\theta$ , while those of  $B \rightarrow K_1(1400)\ell^+\ell^-$  are sensitive to it seriously. We also find that the branching ratios of  $B \rightarrow K_1(1270)\ell^+\ell^-$  are much larger than those of  $B \rightarrow K_1(1400)\ell^+\ell^-$ . For  $B \rightarrow K_1\tau^+\tau^-$ , the branching ratios are very small due to small phase spaces.

Now, we turn to a discussion of the new physics contribution. Within a family non-universal  $Z'$  model, the  $Z'$  contribution to  $B \rightarrow K_1\ell^+\ell^-$  decay involves four new parameters  $|B_{sb}^L|$ ,  $\phi_s^L$ ,  $B_{\ell\ell}^L$  and  $B_{\ell\ell}^R$ . The tasks of constraining the above parameters from the well measured channels have been done by many groups in the past few years. Combining the constraints from  $\bar{B}_s - B_s$  mixing,  $B \rightarrow \pi K^{(*)}$  and  $\rho K$  decays,  $|B_{sb}^L|$  and  $\phi_s^L$  have been strictly constrained by Chang *et al.* [21]. They also performed the constraints of  $B_{ll}^{L,R}$  from  $B \rightarrow X_s\mu^+\mu^-$ ,  $K\mu^+\mu^-$  and  $K^*\mu^+\mu^-$ , as well as  $B_s \rightarrow \mu^+\mu^-$  decay. Recently, there have been more data from Tevatron and LHC on decay processes mentioned above. Many of them might afford stronger upper bounds than before, but the new parameters have not been fitted and we will leave it as our future work. In the current work, we will adopt the parameters fitted in Ref [21] so as to probe contribution of new physics with the largest possibility. For convenience, we recollect their numerical results in the Table V, where S1 and S2 correspond to UTfit collaboration's two fitting results for  $\bar{B}_s - B_s$  mixing [33]. Meanwhile, in order to show the maximal strength of  $Z'$ , with permitted range in S1, we choose the extreme values

$$|B_{sb}^L| = 1.31 \times 10^{-3}, \phi_s^L = -79^\circ, S_{ll} = -6.7 \times 10^{-2}, D_{ll} = -9.3 \times 10^{-2}, \quad (33)$$

and name them as extreme limit values (ELV) expediently.

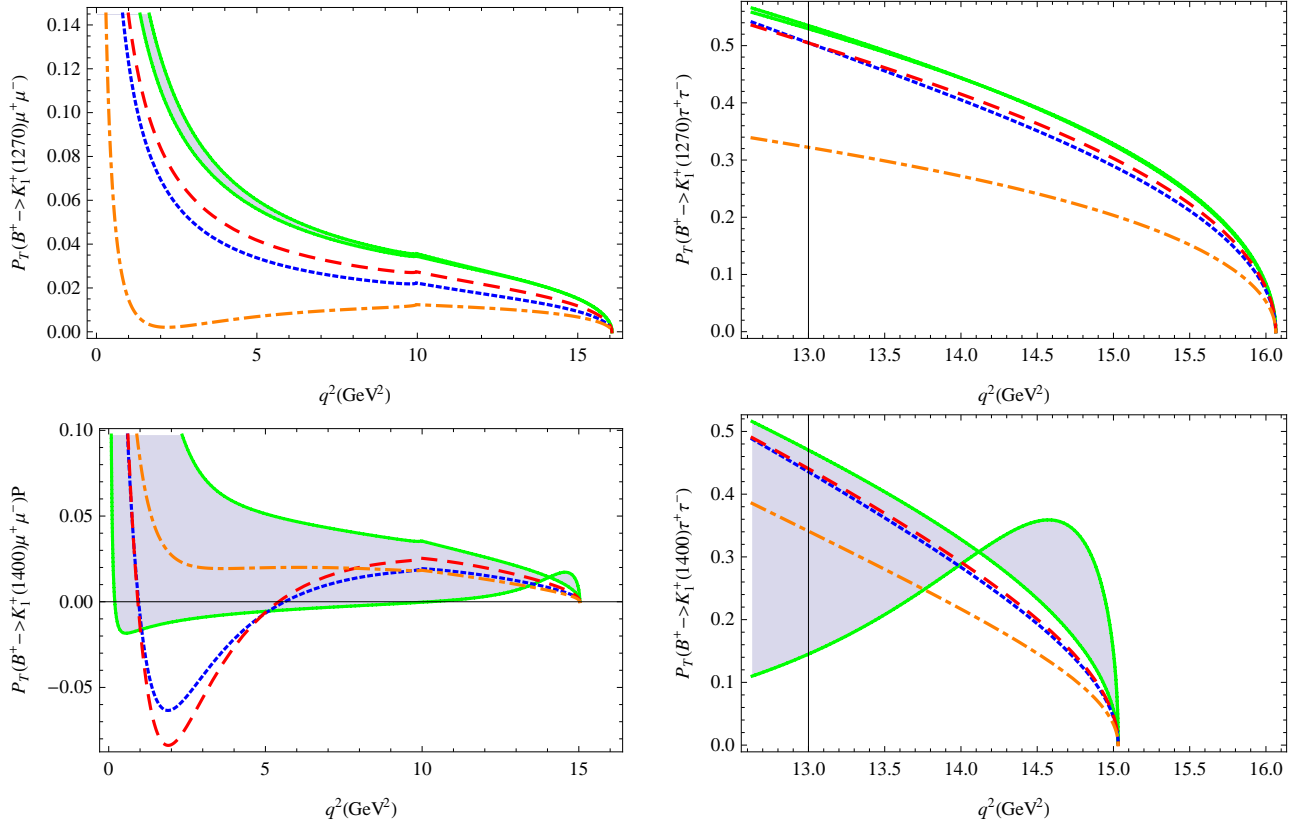


FIG. 5: The transverse lepton polarization asymmetries for the  $B^+ \rightarrow K_1^+ \ell^+ \ell^-$  decays as functions of  $q^2$  (in units of  $\text{GeV}^2$ ).

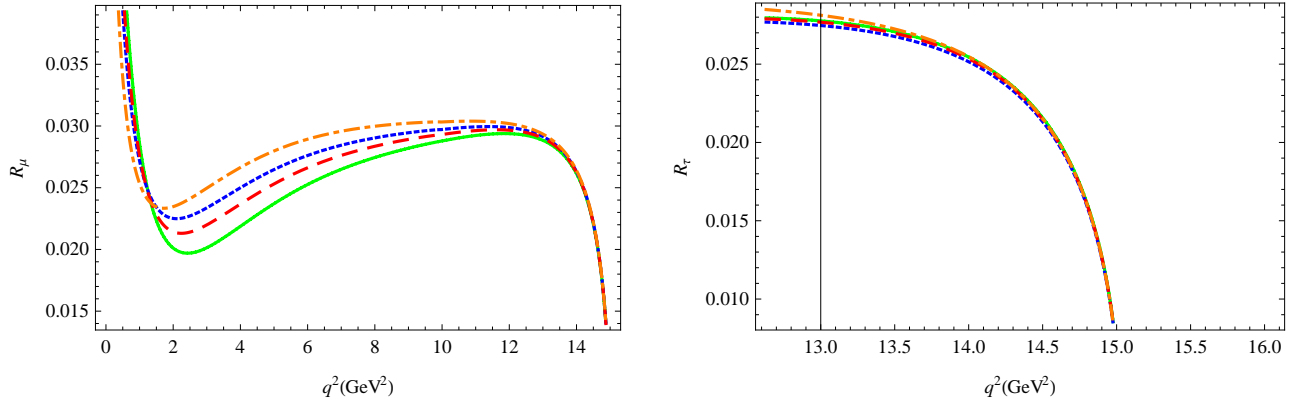


FIG. 6: The ratio of the decay distributions,  $R_\mu$  (left panel) and  $R_\tau$  (right panel), as a function of the dilepton invariant mass  $q^2$  (in units of  $\text{GeV}^2$ ). The legends are the same as in Fig. 2

Considering the  $Z'$  contribution with two sets of parameters, we calculate the non-resonant branching ratios of concerned decay modes and tabulate them in the third and fourth columns of the Table.IV, where the first errors come from the mixing angle  $\theta$  and the second errors are from all uncertainties of  $Z'$  model by adding all the theoretical errors in quadrature. With the ELV parameters, the extreme results are listed in the last column of Table.IV, and the errors are only from mixing angle.

In Fig.2-5, we plot the differential branching ratios, forward-backward asymmetries and polarization asymmetries of the

leptons of  $B^+ \rightarrow K_1(1270)^+\ell^+\ell^-$  and  $B^+ \rightarrow K_1(1400)^+\ell^+\ell^-$ , respectively. In all figures, the bands with solid (green) lines are results from the standard model with  $\theta = -(34 \pm 13)^\circ$ , and dotted (blue), dashed (red) and dot-dashed (orange) lines represent the results with the S1, S2 and ELV parameters by fixing  $\theta = -34^\circ$ , respectively. Some discussions of the above results are in order.

- From the Table. IV, we find that the effect of S1 is more significant than that of S2. For the central values, compared with predictions of the SM, the branching ratio of  $B^- \rightarrow K_1(1270)^-\mu^+\mu^-$  can be enhanced about by 48% in S1, and by 23% in S2. If we choose the extreme limit of S1, the branching ratio can be enhanced one time at most by new physics contribution of  $Z'$ . As concerns  $B \rightarrow K_1(1400)\ell^+\ell^-$ , their branching ratios are more sensitive to the mixing angle than to a new physics contribution, and then it is very hard to differentiate the  $Z'$  effects.
- For the dilepton invariant mass spectrum of  $B^- \rightarrow K_1(1270)^-\mu^+\mu^-$ , the effects of the  $Z'$  boson are quite distinctive from that of the SM, as shown in Fig.2. The reason for the enlargement is the relative change of the absolute values of  $C_9^{\text{eff}}$  and  $C_{10}$ , though the latter is  $q^2$  independent. For  $B^- \rightarrow K_1(1400)^-\mu^+\mu^-$ ,  $Z'$  boson could change the shape effectively, however this contribution would be clouded by the uncertainties from the mixing angle. For the tauon modes, with large tauon mass and small phase space, it is very difficult to disentangle the new physics contribution from the predictions of SM, unless choosing the extreme limit case.
- We plot the normalized forward-backward asymmetries in Fig.3. For  $B \rightarrow K_1\mu^+\mu^-$ , there exist zero crossing positions in SM, S1 and S2. We would like to emphasize that the hadronic uncertainties and mixing angle almost have no influence on zero crossing positions, as shown in figures. Specifically, for  $B \rightarrow K_1(1270)\mu^+\mu^-$ , the zero crossing  $s_0$  positions are 2.3 GeV, 3.3 GeV and 2.9 GeV in SM, S1 and S2. Accordingly, for  $B \rightarrow K_1(1400)\mu^+\mu^-$ ,  $s_0 = 2.8$  GeV, 3.5 GeV, 3.2 GeV. It is obvious that  $s_0$  moves to the positive direction with the  $Z'$  boson effects. And in the limit values, the zero crossing positions disappear. Thus, the measurement of zero position is very important for searching for new physics contribution in the experiments. For  $B \rightarrow K_1(1400)\tau^+\tau^-$ , with the central value of S1 and S2, the forward-backward asymmetries are almost the same as the predictions from SM. However, these asymmetries become almost zero in both low and large momentum regions in the ELV case.
- Just like the  $BR$  and  $A_{FB}$ , the polarization asymmetries of leptons are also good observables for probing the new physics signals. In order to show the effects due to the  $Z'$ , we figure out the longitudinal  $P_L$  and transverse  $P_T$  polarization asymmetries as functions of  $q^2$  in Fig.4 and Fig.5, respectively. The  $P_N$  parts are too tiny to be measured experimentally even in the designed Super-B factory, so we will not discuss them in this work. In the case of  $B \rightarrow K_1(1270)\mu^+\mu^-$ , the longitudinal (transverse) polarization asymmetry of lepton is enhanced (decreased) remarkably by new physics effects. In SM, the longitudinal polarization asymmetry for muon is around  $-1$  in the large momentum region, while it changes to  $-0.6(-0.7)$  in S1 (S2). In the  $Z'$  model, a large value of differential decay rate will suppress the absolute value of longitudinal polarization asymmetry in the large  $q^2$  part. With the extreme values,  $P_L$  flips the sign in the low  $q^2$  region and approaches to zero in the large  $q^2$  region. If there exist large  $Z' - b - s$  and  $Z' - l - l$  couplings, we can check them by measuring the above observables. Similar effects can be found in tau modes, but the deviations are too small to be measured experimentally.
- From the Table.IV, we obtain  $Br(B \rightarrow K_1(1270)\ell^+\ell^-) \gg Br(B \rightarrow K_1(1400)\ell^+\ell^-)$ . It should be helpful to define the ratio

$R_\ell$ , as mentioned in Ref.[1],

$$R_\ell \equiv \frac{d\Gamma(B^- \rightarrow K_1^-(1400)\ell^+\ell^-)/ds}{d\Gamma(B^- \rightarrow K_1^-(1270)\ell^+\ell^-)/ds}. \quad (34)$$

To cross check this conclusion that the ratios are insensitive to new physics contribution, we presented the  $R_\mu$  and  $R_\tau$  as functions of  $q^2$  in Fig. 6, where the solid (green), and dotted (blue), dashed (red) and dot-dashed (orange) lines represent results from the standard model, S1, S2 and ELV parameters, respectively. We show that  $R_\ell(\ell = \mu, \tau)$  are almost unchanged, so that they are not suitable for searching for  $Z'$  effects. These results confirm the conclusion in Ref.[1].

#### IV. SUMMARY

A new family non-universal  $Z'$  boson could be naturally derived in many extensions of SM. One of the possible way to get such non-universal  $Z'$  boson is to include an addition  $U'(1)$  gauge symmetry, which has been studied by many groups. With the data, people had fitted two sets of coupling constants, S1 and S2 namely. In this work, we have considered the contributions of family non-universal  $Z'$  model at the tree level in semi-leptonic  $B$  decays involving axial-vector meson  $K_1$  in the final states. The strange axial-vector mesons,  $K_1(1270)$  and  $K_1(1400)$ , are the mixtures of the  $K_{1A}$  and  $K_{1B}$ , which are the  $1^3P_1$  and  $1^1P_1$  states, respectively. We show that the mixing angle could be constrained by measuring some observables of  $B \rightarrow K_1(1400)\ell^+\ell^-$ , such as the normalized differential forward-backward asymmetry and longitudinal lepton polarization asymmetry. With  $\theta = -34^\circ$ , the branching ratio of  $B \rightarrow K_1(1270)\mu^+\mu^-$  is enhanced about by 50% (30%) with respect to the corresponding SM values by  $Z'$  in S1 (S2). We also found FBA and lepton polarization asymmetries show quite significant discrepancies with respect to the SM values. The zero crossing position in the FBA spectrum at low dilepton mass will move to the positive direction with  $Z'$  boson contribution. We also note that  $B \rightarrow K_1(1400)\mu^+\mu^-$  is not suitable to probe new physics, which will be buried by the uncertainty from the mixing angle. While for the tauon modes, the new physics contributions are not remarkable due to small phase spaces except in the extreme limit. These results could be tested in the running LHC-b experiment and designed Super-B factory.

#### Acknowledgement

The work of Y. Li is supported in part by the NSFC ((Nos.10805037 and 11175151)) and the Natural Science Foundation of Shandong Province (ZR2010AM036). K. C. Y. is supported in part by the National Center for Theoretical Sciences and the National Science Council of R.O.C. under Grant No. NSC99-2112-M-003-005-MY3.

#### Appendix

$$\mathcal{A}^{K_1}(\hat{s}) = \frac{2}{1 + \hat{m}_{K_1}} C_9^{\text{eff}}(\hat{s}) A^{K_1}(\hat{s}) + \frac{4\hat{m}_b}{\hat{s}} C_7^{\text{eff}} T_1^{K_1}(\hat{s}), \quad (35)$$

$$\mathcal{B}^{K_1}(\hat{s}) = (1 + \hat{m}_{K_1}) \left[ C_9^{\text{eff}}(\hat{s}) V_1^{K_1}(\hat{s}) + \frac{2\hat{m}_b}{\hat{s}} (1 - \hat{m}_{K_1}) C_7^{\text{eff}} T_2^{K_1}(\hat{s}) \right], \quad (36)$$

$$\mathcal{C}^{K_1}(\hat{s}) = \frac{1}{1 - \hat{m}_{K_1}^2} \left[ (1 - \hat{m}_{K_1}) C_9^{\text{eff}}(\hat{s}) V_2^{K_1}(\hat{s}) + 2\hat{m}_b C_7^{\text{eff}} \left( T_3^{K_1}(\hat{s}) + \frac{1 - \hat{m}_{K_1}^2}{\hat{s}} T_2^{K_1}(\hat{s}) \right) \right],$$

$$\mathcal{D}^{K_1}(\hat{s}) = \frac{1}{\hat{s}} \left[ C_9^{\text{eff}}(\hat{s}) \left\{ (1 + \hat{m}_{K_1}) V_1^{K_1}(\hat{s}) - (1 - \hat{m}_{K_1}) V_2^{K_1}(\hat{s}) - 2\hat{m}_{K_1} V_0^{K_1}(\hat{s}) \right\} - 2\hat{m}_b C_7^{\text{eff}} T_3^{K_1}(\hat{s}) \right], \quad (37)$$

$$\mathcal{E}^{K_1}(\hat{s}) = \frac{2}{1 + \hat{m}_{K_1}} C_{10} A^{K_1}(\hat{s}), \quad (39)$$

$$\mathcal{F}^{K_1}(\hat{s}) = (1 + \hat{m}_{K_1}) C_{10} V_1^{K_1}(\hat{s}), \quad (40)$$

$$\mathcal{G}^{K_1}(\hat{s}) = \frac{1}{1 + \hat{m}_{K_1}} C_{10} V_2^{K_1}(\hat{s}), \quad (41)$$

$$\mathcal{H}^{K_1}(\hat{s}) = \frac{1}{\hat{s}} C_{10} \left[ (1 + \hat{m}_{K_1}) V_1^{K_1}(\hat{s}) - (1 - \hat{m}_{K_1}) V_2^{K_1}(\hat{s}) - 2\hat{m}_{K_1} V_0^{K_1}(\hat{s}) \right]. \quad (42)$$

- 
- [1] H. Hatanaka and K. C. Yang, Phys. Rev. D **78**, 074007 (2008) [arXiv:0808.3731 [hep-ph]].
- [2] R. H. Li, C. D. Lu and W. Wang, Phys. Rev. D **79**, 094024 (2009) [arXiv:0902.3291 [hep-ph]].
- [3] M. A. Paracha, I. Ahmed and M. J. Aslam, Eur. Phys. J. C **52**, 967 (2007) [arXiv:0707.0733 [hep-ph]].
- [4] V. Bashiry, JHEP **0906**, 062 (2009) [arXiv:0902.2578 [hep-ph]].
- [5] I. Ahmed, M. A. Paracha and M. J. Aslam, Eur. Phys. J. C **54**, 591 (2008) [arXiv:0802.0740 [hep-ph]];  
A. Saddique, M. J. Aslam and C. D. Lu, Eur. Phys. J. C **56**, 267 (2008) [arXiv:0803.0192 [hep-ph]];  
I. Ahmed, M. A. Paracha and M. J. Aslam, Eur. Phys. J. C **71**, 1521 (2011) [arXiv:1002.3860 [hep-ph]].
- [6] V. Bashiry and K. Azizi, JHEP **1001**, 033 (2010) [arXiv:0903.1505 [hep-ph]].
- [7] A. Ahmed, I. Ahmed, M. A. Paracha and A. Rehman, arXiv:1105.3887 [hep-ph].
- [8] M. Suzuki, Phys. Rev. D **47**, 1252 (1993).
- [9] L. Burakovsky and J. T. Goldman, Phys. Rev. D **57**, 2879 (1998) [arXiv:hep-ph/9703271].
- [10] H. Y. Cheng, Phys. Rev. D **67**, 094007 (2003) [arXiv:hep-ph/0301198].
- [11] H. Hatanaka and K. C. Yang, Phys. Rev. D **77**, 094023 (2008) [arXiv:0804.3198 [hep-ph]].
- [12] H. Dag, A. Ozpineci and M. T. Zeyrek, J. Phys. G **38**, 015002 (2011) [arXiv:1001.0939 [hep-ph]];  
M. Bayar and K. Azizi, Eur. Phys. J. C **61**, 401 (2009) [arXiv:0811.2692 [hep-ph]].
- [13] K. C. Yang, Phys. Rev. D **78**, 034018 (2008) [arXiv:0807.1171 [hep-ph]].
- [14] R. H. Li, C. D. Lu and W. Wang, Phys. Rev. D **79**, 034014 (2009) [arXiv:0901.0307 [hep-ph]].
- [15] H. Y. Cheng and C. K. Chua, Phys. Rev. D **81**, 114006 (2010) [arXiv:0909.4627 [hep-ph]];  
R. C. Verma, arXiv:1103.2973 [hep-ph].
- [16] G. Buchalla, G. Burdman, C. T. Hill and D. Kominis, Phys. Rev. D **53**, 5185 (1996) [arXiv:hep-ph/9510376].
- [17] E. Nardi, Phys. Rev. D **48**, 1240 (1993) [arXiv:hep-ph/9209223].
- [18] P. Langacker and M. Plumacher, Phys. Rev. D **62**, 013006 (2000) [arXiv:hep-ph/0001204].
- [19] V. Barger, *et. al*, Phys. Lett. B **580**, 186 (2004) [arXiv:hep-ph/0310073];  
V. Barger, *et. al*, Phys. Lett. B **598**, 218 (2004) [arXiv:hep-ph/0406126];  
V. Barger, *et. al*, arXiv:0906.3745 [hep-ph];  
V. Barger, *et. al*, Phys. Rev. D **80**, 055008 (2009) [arXiv:0902.4507 [hep-ph]].
- [20] K. Cheung, *et. al*, Phys. Lett. B **652**, 285 (2007) [arXiv:hep-ph/0604223];  
C. W. Chiang, *et. al*, JHEP **0608**, 075 (2006) [arXiv:hep-ph/0606122];  
C. H. Chen and H. Hatanaka, Phys. Rev. D **73**, 075003 (2006) [arXiv:hep-ph/0602140];  
C. H. Chen, arXiv:0911.3479 [hep-ph];

- C. W. Chiang, R. H. Li and C. D. Lu, arXiv:0911.2399 [hep-ph];  
 R. Mohanta and A. K. Giri, Phys. Rev. D **79**, 057902 (2009) [arXiv:0812.1842 [hep-ph]];  
 J. Hua, C. S. Kim and Y. Li, Phys. Lett. B **690**, 508 (2010) [arXiv:1002.2532 [hep-ph]];  
 J. Hua, C. S. Kim and Y. Li, Eur. Phys. J. C **69**, 139 (2010) [arXiv:1002.2531 [hep-ph]].
- [21] Q. Chang, X. Q. Li and Y. D. Yang, JHEP **0905**, 056 (2009) [arXiv:0903.0275 [hep-ph]];  
 Q. Chang, X. Q. Li and Y. D. Yang, JHEP **1002**, 082 (2010) [arXiv:0907.4408 [hep-ph]];  
 Q. Chang, X. Q. Li and Y. D. Yang, JHEP **1004**, 052 (2010) [arXiv:1002.2758 [hep-ph]];  
 Q. Chang and Y. H. Gao, Nucl. Phys. B **845**, 179 (2011) [arXiv:1101.1272 [hep-ph]].
- [22] P. Langacker, arXiv:0801.1345 [hep-ph].
- [23] J.Dickens, V.Gibon, C.Lazzeroni and M.Patel, CERN-LHCB-2007-038;  
 J.Dickens, V.Gibon, C.Lazzeroni and M.Patel, CERN-LHCB-2007-039.
- [24] B. Aubert *et al.* [BABAR Collaboration], Phys. Rev. Lett. **91**, 221802 (2003) [arXiv:hep-ex/0308042];  
 B. Aubert *et al.* [BABAR Collaboration], Phys. Rev. D **73**, 092001 (2006) [arXiv:hep-ex/0604007];  
 B. Aubert *et al.* [BABAR Collaboration], Phys. Rev. D **79**, 031102 (2009) [arXiv:0804.4412 [hep-ex]];  
 I. Adachi *et al.* [Belle Collaboration], arXiv:0810.0335 [hep-ex].
- [25] M. O. Bettler [LHCb Collaboration], arXiv:0910.0942 [hep-ex].
- [26] K. Nakamura *et al.* (Particle Data Group), J. Phys. G **37**, 075021. (2010)
- [27] G. Buchalla, A. J. Buras and M. E. Lautenbacher, Rev. Mod. Phys. **68**, 1125 (1996) [arXiv:hep-ph/9512380].
- [28] C.S. Kim, T. Morozumi, A.I. Sanda, Phys. Lett. B **218** (1989) 343;  
 X. G. He, T. D. Nguyen and R. R. Volkas, Phys. Rev. D **38** (1988) 814;  
 B. Grinstein, M.J. Savage, M.B. Wise, Nucl. Phys. B **319** (1989) 271;  
 N. G. Deshpande, J. Trampetic and K. Panose, Phys. Rev. D **39** (1989) 1461;  
 P. J. O'Donnell and H. K. K. Tung, Phys. Rev. D **43** (1991) 2067;  
 N. Paver and Riazuddin, Phys. Rev. D **45** (1992) 978;  
 A. Ali, T. Mannel and T. Morozumi, Phys. Lett. B **273** (1991) 505;  
 D. Melikhov, N. Nikitin and S. Simula, Phys. Lett. B **430** (1998) 332 [arXiv:hep-ph/9803343];  
 J. M. Soares, Nucl. Phys. B **367** (1991) 575;  
 G. M. Asatrian and A. Ioannisian, Phys. Rev. D **54** (1996) 5642 [arXiv:hep-ph/9603318].
- [29] A. J. Buras, M. Misiak, M. Munz and S. Pokorski, Nucl. Phys. B **424** (1994) 374 [hep-ph/9311345].
- [30] M. Beneke, G. Buchalla, M. Neubert, C. T. Sachrajda, Eur. Phys. J. C **61** (2009) 439 [arXiv:0902.4446 [hep-ph]];  
 M. Bartsch, M. Beylich, G. Buchalla, D. N. Gao, JHEP **0911** (2009) 011 [arXiv:0909.1512 [hep-ph]];  
 A. Khodjamirian, T. Mannel, A. A. Pivovarov and Y. M. Wang, JHEP **1009**, 089 (2010) [arXiv:1006.4945 [hep-ph]].
- [31] K. G. Chetyrkin, M. Misiak and M. Munz, Phys. Lett. B **400** (1997) 206 [Erratum-ibid. B **425** (1998) 414] [hep-ph/9612313].
- [32] W. Altmannshofer, P. Ball, A. Bharucha, A. J. Buras, D. M. Straub and M. Wick, JHEP **0901** (2009) 019 [arXiv:0811.1214 [hep-ph]].
- [33] M. Bona *et al.*, arXiv:0906.0953 [hep-ph];  
 M. Bona *et al.* [UTfit Collaboration], PMC Phys. A **3**, 6 (2009) [arXiv:0803.0659 [hep-ph]].